Paper:
Zong, H., Lou, Y., Li, M., Wang, K., Jain, S. & Wang, Z. (2019). Improved open-circuit voltage via Cs2CO3-Doped TiO2 for high-performance and stable perovskite solar cells. *Organic Electronics*, 105495
http://dx.doi.org/10.1016/j.orgel.2019.105495

Journal Pre-proof

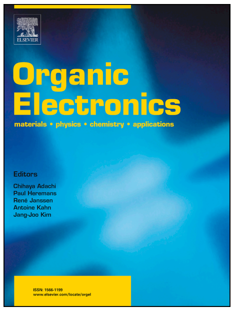

Improved open-circuit voltage via Cs_2CO_3-Doped TiO_2 for high-performance and stable perovskite solar cells

Hao Zong, Yan-Hui Lou, Meng Li, Kai-Li Wang, Sagar M. Jain, Zhao-Kui Wang

PII: S1566-1199(19)30522-1

DOI: https://doi.org/10.1016/j.orgel.2019.105495

Reference: ORGELE 105495

To appear in: *Organic Electronics*

Received Date: 16 August 2019

Revised Date: 20 September 2019

Accepted Date: 8 October 2019

Please cite this article as: H. Zong, Y.-H. Lou, M. Li, K.-L. Wang, S.M. Jain, Z.-K. Wang, Improved open-circuit voltage via Cs_2CO_3-Doped TiO_2 for high-performance and stable perovskite solar cells, *Organic Electronics* (2019), doi: https://doi.org/10.1016/j.orgel.2019.105495.

Graphic Abstract

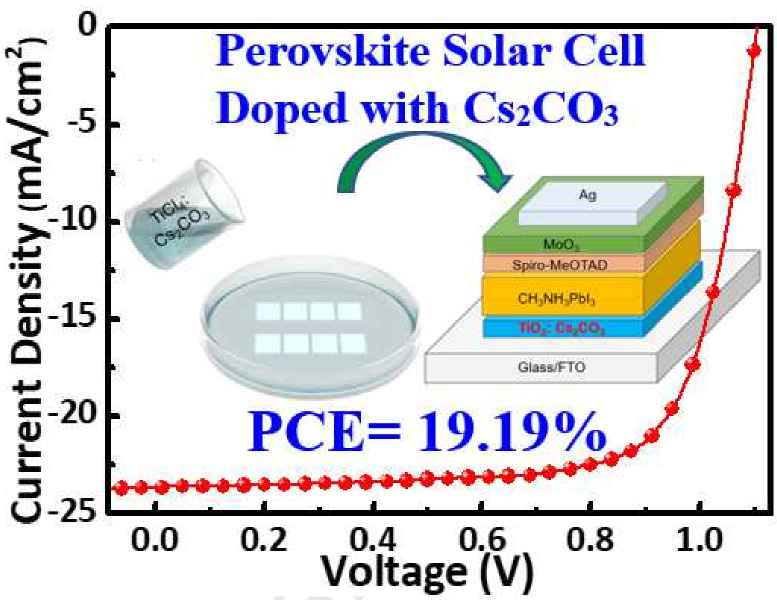

Hao Zong[a], *Yan-Hui Lou*[b,]*, *Meng Li*[a], *Kai-Li Wang*[a], *Sagar M. Jain*[c,]*, *and Zhao-Kui Wang*[a,]*

[a] Institute of Functional Nano & Soft Materials (FUNSOM), Jiangsu Key Laboratory for Carbon-Based Functional Materials & Devices, Soochow University, Suzhou, Jiangsu 215123, China.

[b] College of Physics, Optoelectronics and Energy & Collaborative Innovation Center of Suzhou Nano Science and Technology, Soochow University, Suzhou 215006, China.

[c] SPECIFIC, College of Engineering, Swansea University Bay Campus, Fabian Way, SA1 8EN Swansea, UK

*Corresponding Authors:

yhlou@suda.edu.cn (Y. H. Lou). s.m.jain@swansea.ac.uk (S. M. Jain). zkwang@suda.edu.cn (Z. K. Wang)

Organic-inorganic metal halide perovskites have drawn the interest of scientific community due to their suitable optoelectronic properties and high solar cell efficiency. In this report, we demonstrated, for the first time, the application of Cs_2CO_3 - doped TiO_2 as an efficient electron-transporting layer (ETL) in PSCs. Remarkably, the optimized Cs_2CO_3-doped TiO_2 films exhibited improved wetting properties which assisted the deposition of perovskite films and improved the TiO_2 / perovskite interface by lowering the work function. With X-ray diffraction studies, better crystalline of the perovskite films could be found in the doped devices. Solar cells prepared with the Cs_2CO_3-doped TiO_2 as ETL resulted in a 19% efficiency performance and improved stability.

KEYWORDS: Perovskite solar cells; Cs_2CO_3; TiO_2; Electron-transporting; Stability.

fossil fuels and environmental sustainability issues. Moreover, the ever-increasing human population has resulted in high energy demands. Among all renewable energy sources, photovoltaic energy stands out and is most widely investigated. Recently, the perovskite solar cells (PSCs) have come into limelight due to their ease of fabrication and rapid improvement in performance (which is currently comparable to those of polycrystalline silicon solar cells). Interestingly, PSCs unlike silicon solar cells, can be transparent, laminated and even be fabricated on flexible substrates.[1-3] Since the first fabrication of PSCs by Kojima et al. yielded a power conversion efficiency (PCE) of 3.81% in 2009,[4] researchers have made steady improvements in the PCE, which has now exceeded 25%.[5, 6] PSCs efficiency is improved by varieties of methods such as employing new perovskite absorber materials, fine-tuning the chemical composition, controlling the morphology of the film,[7] and modifying the interface. [8-16] Titanium dioxide (TiO_2) emerged as most conventional electron transport layer in perovskite solar cells. However, there exists still possibilities to improve its charge mobility and defect properties (oxygen vacancies). [17] Unfortunately, very few studies reported in this direction. Cesium carbonate (Cs_2CO_3) which could be solution-processed due to its excellent solubility in polar solvents has been extensively used as a surface modification material in organic light emitting diodes (OLEDs) and solar cells (OSCs) to improve electron-injection from the metal cathode and as dopant in an electron transport layer.[18-21]

Here, we demonstrated for the first time, the use of Cs_2CO_3 as a dopant in TiO_2 layer. Cs_2CO_3 which is reported to be a surface modification material with a work function lower than that of TiO_2 have the ability to reduce the work function of electron transporting layer (ETL).[19] Cs_2CO_3 when used as a modification material can fine-tune the mesoporous performance with a PCE > 19%. This is much improved efficiency compared to the 17% PCE obtained from PSCs fabricated with conventional mesoporous TiO_2 electron transport layers. It is observed from X-ray diffraction and UV-absorbance measurements that the perovskite films deposited on Cs_2CO_3-doped TiO_2 resulted into good quality perovskite films which is a result of improved wetting properties of Cs_2CO_3-doped TiO_2.

2. Experimental Details

2.1 Material and Solution Preparation

The Solar cells are fabricated on fluorine-doped tin oxide (FTO) covered glass substrates (Pilkington, Nippon Sheet Glass). Titanium tetrachloride ($TiCl_4$), 4-tert-butyl pyridine (tBP) and Lithium bis (trifluoromethanesulfonyl) imide (Li-TFSI) were obtained from Sigma-Aldrich. Spiro-OMeTAD were obtained from 1-Material Ltd. Lead iodide (PbI_2, 99.99%), methylammonium iodide (MAI)，dimethyl sulfoxide (DMSO), cesium carbonate (Cs_2CO_3), chlorobenzene (CB) and γ-butyrolactone (GBL) were obtained from Alfa Aesar Ltd. Perovskite precursor solution was prepared by mixing 190 mg CH_3NH_3I and 512 mg (PbI_2) powder in 1 mL γ-butyrolactone and dimethylsulfoxide (7:3, v/v). Spiro-OMeTAD solution was prepared by mixing 36 μL 4-tert-butylpyridine and 22.5 μL Li-TFSI solution (520 mg Li-TFSI in 1 mL acetonitrile) in 1 mL chlorobenzene solution with 90 mg Spiro-OMeTAD.

2.2 Device Fabrication

Deionized water, acetone and ethanol were used to clean the FTO glass substrates thoroughly. The cleaned FTO glass substrates were treated under ultraviolet (UV) irradiation at an elevated temperature for 30 min. TiO_2 compact layer was deposited on the substrates using a 200 mL $TiCl_4$ solution doped with Cs_2CO_3 at 70 °C for 1 hour. The doped TiO_2 layer was

2000 and 4000 rpm for 20 and 40 s respectively. 150 μL chlorobenzene (antisolvent) was dropped onto the substrate, 20 sec into the second step. The substrates were annealed at 100 □ for 10 min and allowed to cool to room temperature. The perovskite layers were then coated with spiro-OMeTAD solution at 5000 rpm for 40s. Finally, MoO_3 and Ag were thermally and sequentially evaporated onto the devices under a pressure of 4×10^{-6} Torr through a shadow mask with an active area of 0.09 cm^2.

J-V curves of the PSCs were acquired by operating a Keithley 2400 source meter under Air Mass (AM 1.5 G) solar irradiation at 100 mW/cm^2 (Newport, Class AAA solar simulator, 94023A-U) under 1 sun illumination. The field-emission scanning electron microscope (SEM) images were acquired from a Quanta 200 FEG. AFM images were acquired on a Veeco Multimode V instrument to observe the morphology of TiO_2 films. X-ray diffraction (XRD) patterns were obtained using PANalytical (Empyrean) equipment. The absorbance of the different perovskite films was measured on an UV–vis spectrophotometer (PerkinElmer Lambda 750). The UPS patterns were obtained through the assistance of Jinan University.

3. Results and Discussion

Fig. 1 shows the schematic illustration of the fabrication of devices with and without Cs_2CO_3 doped TiO_2 layer as ETL. For the doped ETL device. Cs_2CO_3 was added into $TiCl_4$ solution in a chemical bath to yield the Cs_2CO_3 doped TiO_2 layer. Subsequent processes which including perovskite, Spiro-OMeTAD and electrode deposition followed the same methods for both devices. From Fig. S6, pH of the prepared $TiCl_4$ solutions increased with increasing doping concentration. For example, the pH was 1.73 without Cs_2CO_3, 2.21 with 1 mg/ml Cs_2CO_3 and 2.45 with 2 mg/ml Cs_2CO_3. Crystallization needs to occur in an ideal pH environment as higher or lower pH may be unfavorable.[22] Also, sheet resistances were

Fig. 2 shows Atomic Force Microscope (AFM) images of surface topographies of TiO_2 layers with/without Cs_2CO_3 doping. The root-mean-square (RMS) roughness peaked at 5.90 nm at a Cs_2CO_3 doping concentration of 1 mg/ml. Different doping concentrations of Cs_2CO_3 gave variable surface RMS. For doping concentrations lower than 1 mg/ml, the crystallization of Cs_2CO_3 was suppressed. However, higher Cs_2CO_3 concentration $\geq$ 1 mg/ml yielded higher crystallinity and lower RMS.[23] The devices with doped TiO_2 exhibited better photoelectrical performance.

The perovskite solution spin-coated on 0 mg/ml, 1 mg/ml and 2 mg/ml Cs_2CO_3 doped TiO_2 shows contact angles of 66.1°, 58.4° and 60.5°, respectively (Fig. 3a, b, c). Smaller contact angle yields better contact. This demonstrates that the 1 mg/ml Cs_2CO_3 doped TiO_2 shows the best affinity and wetting capability for perovskite films.[24] Doping Cs_2CO_3 (1 mg/ml) into TiO_2 assists in forming a better contact with the spin-coated perovskite layer, giving rise to improved photoelectrical performance.

SEM images of perovskite films spin-coated on the TiO_2 films are presented in Fig. 3d, e, f. In comparison with the film deposited on pristine TiO_2 film, the crystalline grains of the films on doped TiO_2 are much bigger with the 1 mg/ml Cs_2CO_3 doped TiO_2 showing superior crystallinity. It is evident that optimal doping of Cs_2CO_3 into TiO_2 layer increases the crystalline grain size of the perovskite layer. This can be ascribed to improved crystallinity and morphology of the underlying doped-TiO_2. It demonstrates that Cs_2CO_3 could act as a proper surface modification material if appropriate amounts are doped into TiO_2.[25,26]

The crystalline features of the perovskite films were further evaluated by X-ray diffraction (XRD). Fig. 4a and Fig. S2 show the XRD patterns of $CH_3NH_3PbI_3$ films spin-coated on different Cs_2CO_3:TiO_2 layers. Dominant diffraction peak appearing at 14.1°, 28.4° and 32.0° represent (110), (220) and (310) planes of perovskite crystal respectively. Interestingly, a preferential growth along the <110> orientation.[27] Efficient carrier transport and collection can be achieved along the preferential orientation of the perovskite films.

Ultraviolet photoelectron spectroscopy (UPS) was applied to characterize the energy band features of different TiO_2 and perovskite layers. Fig. 5a and b show that effective work function decreases from 5.5 eV to 4.7 eV when the optimal amount of Cs_2CO_3 (1 mg/ml) is doped into TiO_2 layer.[28] As a result, the work function of $CH_3NH_3PbI_3$ layer also decreases as shown in Fig. 5b. The fermi level energy difference which was 2.1 eV before doping changed to 3.2 eV after doping which accounts for the observed change in V_{oc}. The increase in Fermi level of TiO_2 and the larger energy difference, increase the chance of electron injection from absorber layer and induce electron density rise in the ETL. [29] Furthermore, the valence band maximum (VBM) of $CH_3NH_3PbI_3$ increased by 0.7 eV. This may help to decrease the hole extraction barrier and improve device performance.[30] The mobilities of the pristine TiO_2 and doped-TiO_2 thin film were derived from *J-V* curves of electron-only devices with a structure of FTO/TiO_2(with and w/o Cs_2CO_3)/ $CH_3NH_3PbI_3$/PCBM/Ag in Fig. 4b by using the Mott-Gurney Equation ($J = 9\varepsilon_r\varepsilon_0\mu V^2/8d^3$) where ε_r is the dielectric constant of TiO_2, ε_0 is the vacuum permittivity, d is the thickness of TiO_2, V is the applied voltage and μ is the electron mobility. As shown in the Fig. 4b, the the $lgJ - lgV$ curves are not linearly. Take the point where the slope is 2 into consideration. And by using more points, the results will be more accurate. After substitution of several points for computation and averaging the values, the final results were got.[31] The electron mobility of the pristine TiO_2 thin film and the optimal doped-TiO_2 thin film were calculated to be 6.56×10^{-4} cm^2 V^{-1} s^{-1} and 3.01×10^{-3} cm^2 V^{-1} s^{-1}, respectively, indicating that electron transfer efficiency can be improved by doping Cs_2CO_3 into TiO_2 with the proper concentration. And also, we applied the photoluminescence (PL) measurement to determine the charge transport and extraction

(107 ns) than that on the pristine TiO_2 (188 ns). In addition, from Fig. S5, we can find that the thin film on pristine TiO_2 layer has a stronger intensity than that on the doped one in which the carrier extraction is more effective. The results are corresponding to the mobility measurement. To compare the absorption of light in perovskite films deposited on pristine TiO_2 and Cs_2CO_3-doped TiO_2 films, UV-vis absorption spectra (Fig. 4c) between 400 nm and 850 nm were obtained. The perovskite film deposited on doped TiO_2 shows improved absorption. This is because Cs_2CO_3 doping reduces trap states and decreases charge recombination in the TiO_2/perovskite interface, leading to improved performance. The improved performance is also partly due to the superior wetting of perovskite solution on the doped TiO_2 layer and high crystallinity of the perovskite layer. Fig. 4d shows that the transmittances of the pristine and doped TiO_2 film are almost the same, indicating that Cs_2CO_3 doping does not impair the optical properties of the TiO_2 film. However, high concentration Cs_2CO_3 doping is detrimental to the optical properties of the perovskite film as its absorbance decreases.

Finally, to compare the effect of doping Cs_2CO_3 into TiO_2, perovskite solar cells with FTO/TiO_2:Cs_2CO_3/$CH_3NH_3PbI_3$/Spiro-OMeTAD/ MoO_3/Ag architecture were prepared and the device performance compared. Fig. 5c shows the *J-V* curves of the devices prepared using pristine TiO_2 and Cs_2CO_3-doped TiO_2 layers. The *J-V* curves indicate improvement in the voltage and current for the cells prepared with 1 mg/ml Cs_2CO_3-doped-TiO_2 layer. The measurements were developed under the condition where the temperature is 25 °C, the relative humidity is 20% and the with light intensity of 100 mW/cm^2. Table 1 summarizes the photovoltaic parameters of perovskite solar cells. The device made using pristine TiO_2 films show PCE of 17.39%, while the optimal device shows improved PCE of 19.19%. Lower and pristine TiO_2 and 1 mg/ml Cs_2CO_3 doped TiO_2 are presented in Fig. S3. The PSC prepared using the optimized Cs_2CO_3 doping shows better performance and reproducibility. Fig. 5d shows the stability measurement of the solar cells based on pristine TiO_2 and doped-TiO_2 kept for more than 200 hours in ambient without encapsulation. The solar cell based on doped TiO_2 shows better stability. This could be attributed to the improved crystalline. Thus, fabricating PSCs with Cs_2CO_3-doped-TiO_2 as ETL simultaneously improves their stability and efficiency.

4. Conclusions

In summary, we demonstrated a strategy to modify conventional TiO_2 ETL with Cs_2CO_3 doping. Solar cells fabricated using optimal doping concentration of 1 mg/ml resulted in a highest power conversion efficiency of 19.19% and improved stability over 200 hours. The improvement in performance is ascribed to better perovskite film quality formed due to the suitable wetting properties and lower work function of the Cs_2CO_3-doped TiO_2 films. This approach can efficiently modify conventional TiO_2 ETL and improve the stability and performance of PSCs.

Acknowledgements

The authors acknowledge financial support from the National Key R&D Program of China (No. 2016YFA0202402), the Natural Science Foundation of China (Nos. 91733301, 61674109), and the Natural Science Foundation of Jiangsu Province (No. BK20170059). This project is also funded by the Collaborative Innovation Center of Suzhou Nano Science and Technology, the Priority Academic Program Development of Jiangsu Higher Education Institutions (PAPD), and by the “111” Project of The State Administration of Foreign Experts innovation programme under the Marie Skłodowska-Curie grant agreement No 663830.

REFERENCES

[1] C. Roldán-Carmona, O. Malinkiewicz, A. Soriano, G. Mínguez Espallargas, A. Garcia, P. Reinecke, T. Kroyer, M.I. Dar, M.K. Nazeeruddin, H.J. Bolink, Energy Environ. Sci. 7 (2014) 994-997.

[2] G.E. Eperon, V.M. Burlakov, A. Goriely, H.J. Snaith, ACS Nano 8 (2014) 591-598.

[3] H.J. Snaith, J. Phys. Chem. Lett. 4 (2013) 3623-3630.

[4] A. Kojima, K. Teshima, Y. Shirai, T. Miyasaka, J. Am. Chem. Soc. 131 (2009) 6050-6051.

[5] D. Zhao, C. Wang, Z. Song, Y. Yu, C. Chen, X. Zhao, K. Zhu, Y. Yan, ACS Energy Lett 3 (2018) 305-306.

[6] NREL Best Research Cell Efficiencies, https://www.nrel.gov/pv/cell-efficiency.html, (accessed September, 2019).

[7] J. M. Wang, Z. K. Wang, M. Li, K. H. Hu, Y. G. Yang, Y. Hu, X. Y. Gao, L. S. Liao, ACS Appl. Mater. Interfaces. 9 (2017) 13240-13246.

[8] L.-M. Chen, Z. Xu, Z. Hong, Y. Yang, J. Mater. Chem. 20 (2010) 2575-2598.

[9] M. He, F. Qiu, Z. Lin, J. Mater. Chem. 21 (2011) 17039-17048.

[10] M. He, F. Qiu, Z. Lin, J. Phys. Chem. Lett. 4 (2013) 1788-1796.

[11] H.D. Pham, T.T. Do, J. Kim, C. Charbonneau, S. Manzhos, K. Feron, W.C. Tsoi, J.R. Durrant, S.M. Jain, P. Sonar, Adv. Energy Mater. 8 (2018) 1703007.

[12] H.D. Pham, K. Hayasake, J. Kim, T.T. Do, H. Matsui, S. Manzhos, K. Feron, S. Tokito, T. Watson, W.C. Tsoi, N. Motta, J.R. Durrant, S.M. Jain, P. Sonar, J. Mater. Chem. C 6 (2018) 3699-3708.

[13] Z. K. Wang, L. S. Liao, Adv. Optical Mater. 6 (2018) 1800276.

[14] Z. Liu, K. Liu, H. Wang, S.M. Jain, J. Duan, T. He, R. Fan, J. Yang, H. Liu, F. Zhang, Sol. Energy 176 (2018) 1-9.

[15] D. Phuyal, S.M. Jain, B. Philippe, M.B. Johansson, M. Pazoki, J. Kullgren, K.O. Kvashnina, M. Klintenberg, E.M.J. Johansson, S.M. Butorin, O. Karis, H. Rensmo, J. Mater. Chem. A 6 (2018) 9498-9505.

[17] L.-L. Jiang, Z.-K. Wang, M. Li, C.-H. Li, P.-F. Fang, L.-S. Liao, Sol. RRL 2 (2018) 1800149.

[18] C.-W. Chen, Y.-J. Lu, C.-C. Wu, E.H.-E. Wu, C.-W. Chu, Y. Yang, Appl. Phys. Lett. 7 (2005) 241121.

[19] G. Li, C.W. Chu, V. Shrotriya, J. Huang, Y. Yang, Appl. Phys. Lett. 88 (2006) 253503.

[20] L.-P. Lu, D. Kabra, K. Johnson, R.H. Friend, Adv. Funct. Mater. 22 (2011) 144-150.

[21] J. Huang, Z. Xu, Y. Yang, Adv. Funct. Mater. 17 (2007) 1966-1973.

[22] Y. Chen, N. Li, L. Wang, L. Li, Z. Xu, H. Jiao, P. Liu, C. Zhu, H. Zai, M. Sun, W. Zou, S. Zhang, G. Xing, X. Liu, J. Wang, D. Li, B. Huang, Q. Chen, H. Zhou, Nat. Commun. 10 (2019) 1112-1122.

[23] X. Zeng, T. Zhou, C. Leng, Z. Zang, M. Wang, W. Hu, X. Tang, S. Lu, L. Fang, M. Zhou, J. Mater. Chem. A, 5 (2017) 17499-17505.

[24] Q.-Q. Ye, Z.-K. Wang, M. Li, C.-C. Zhang, K.-H. Hu, L.-S. Liao, ACS Energy Lett 3 (2018) 875-882.

[25] C.-C. Zhang, M. Li, Z.-K. Wang, Y.-R. Jiang, H.-R. Liu, Y.-G. Yang, X.-Y. Gao, H. Ma, J. Mater. Chem. A, 5 (2017) 2572-2579.

[26] Z. Liu, T. He, H. Wang, S.M. Jain, K. Liu, J. Yang, N. Zhang, H. Liu, M. Yuan, J. Power Sources 401 (2018) 303-311.

[27] M. Li, Z.K. Wang, M.P. Zhuo, Y. Hu, K.H. Hu, Q.Q. Ye, S.M. Jain, Y.G. Yang, X.Y. Gao, L.S. Liao, Adv. Mater. 30 (2018) 1800258.

[28] M.-F. Xu, Y.-J. Liao, F.-S. Zu, J. Liang, D.-X. Yuan, Z.-K. Wang, L.-S. Liao, J. Mater. Chem. A 2 (2014) 9400-9404.

[29] J. Qiu, Y. Qiu, K. Yan, M. Zhong, C. Mu, H. Yan, S. Yang, Nanoscale, 5 (2013) 3245-3248.

[30] P. Schulz, E. Edri, S. Kirmayer, G. Hodes, D. Cahen, A. Kahn, Energy Environ. Sci. 7 (2014) 1377-1381.

[31] G. Yin, J. Ma, H. Jiang, J. Li, D. Yang, F. Gao, J. Zeng, Z. Liu, S.F. Liu, ACS Appl. Mater. Inter. 9 (2017) 10752-10758.

Figures and Tables

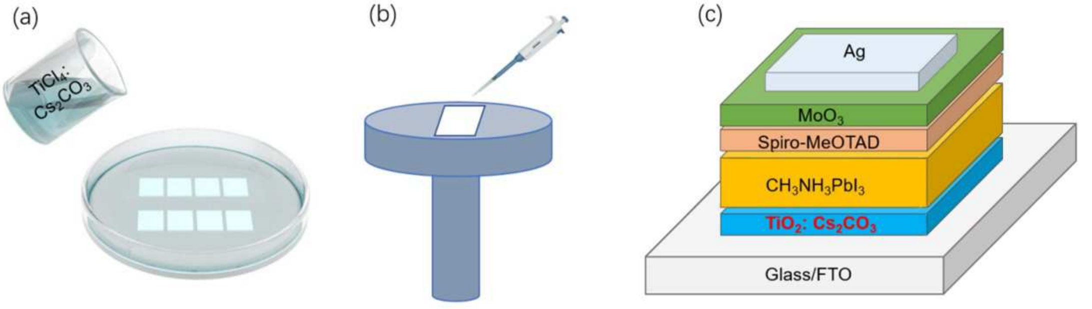

Fig. 1. Schematic diagram for the preparation of devices. (a) Deposition: different concentrations of Cs_2CO_3 are doped in this step. (b) Spin coating: other layers are made by spin-coating. (c) device structure.

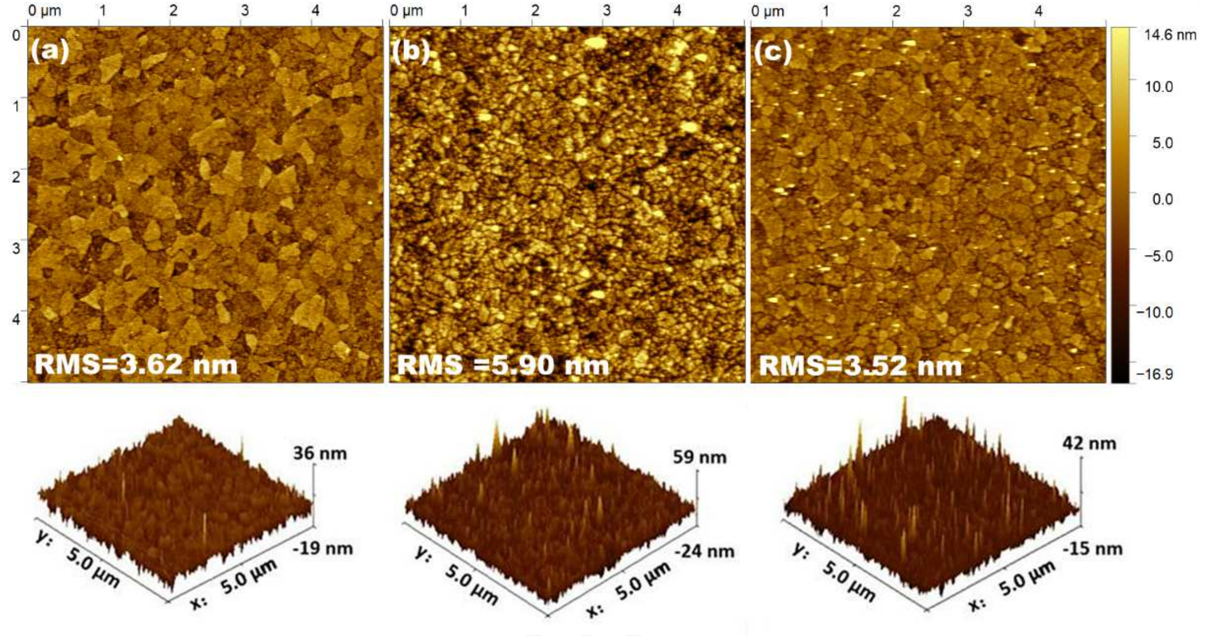

Fig. 2. AFM images of films deposited with different concentrations of Cs_2CO_3 doping. (a) pristine. (b) 1 mg/ml. (c) 2 mg/ml.

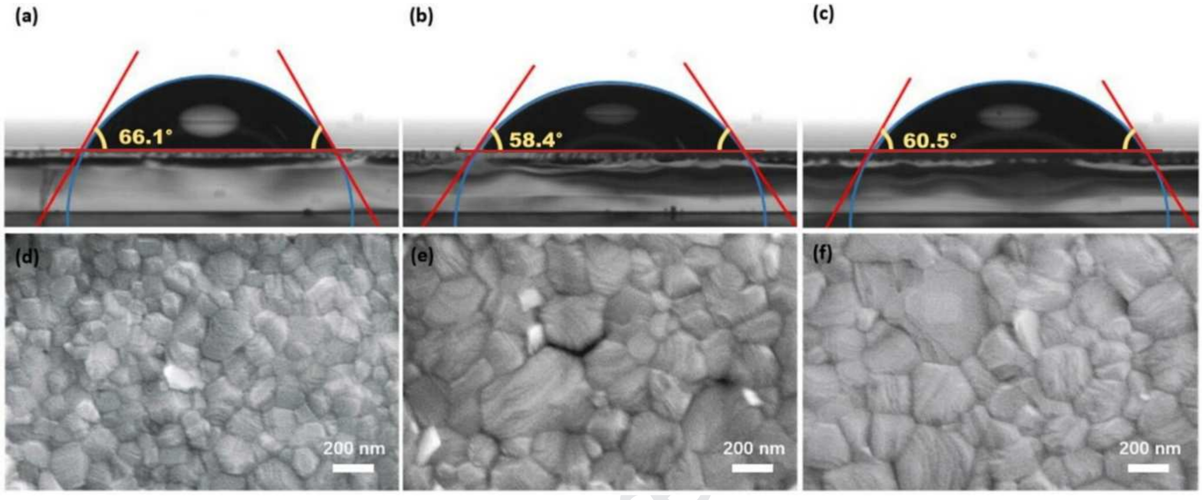

Fig. 3. Contact angles of perovskite solution with different TiO_2 layers (a) pristine. (b) 1 mg/ml. (c) 2 mg/ml. SEM images of perovskite films deposited with different concentrations of Cs_2CO_3. (d)pristine. (e) 1 mg/ml. (f) 2 mg/ml.

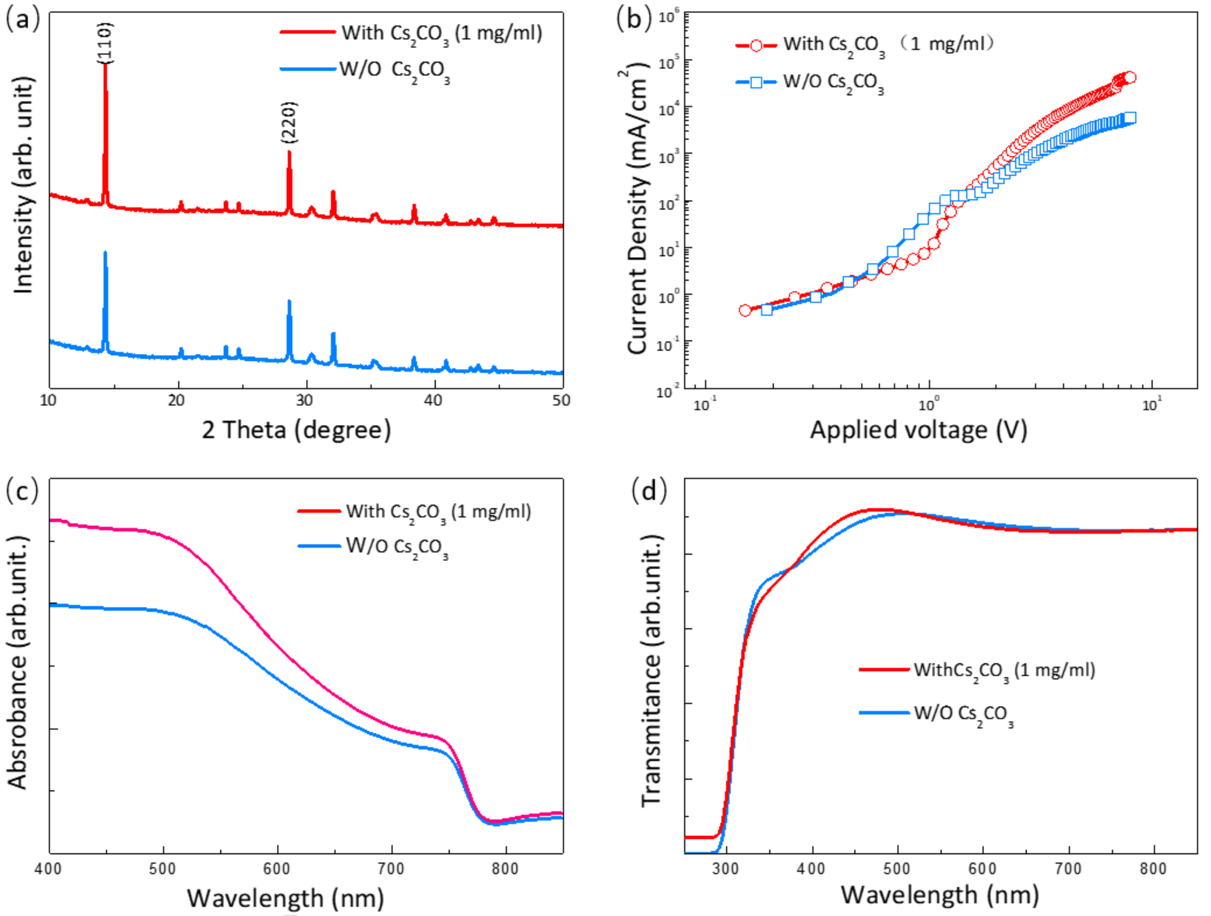

Fig. 4. (a) XRD patterns of $CH_3NH_3PbI_3$ perovskite films with different TiO_2 layers. (b) *J-V* characteristics in electron-only devices with the structure of FTO/TiO_2 (with and W/O Cs_2CO_3)/$CH_3NH_3PbI_3$/PCBM/Ag. (c) UV-vis absorption spectra of the perovskite films without and with Cs_2CO_3 modification. (d) Transmittance spectra of TiO_2 thin film doped with different concentrations of Cs_2CO_3.

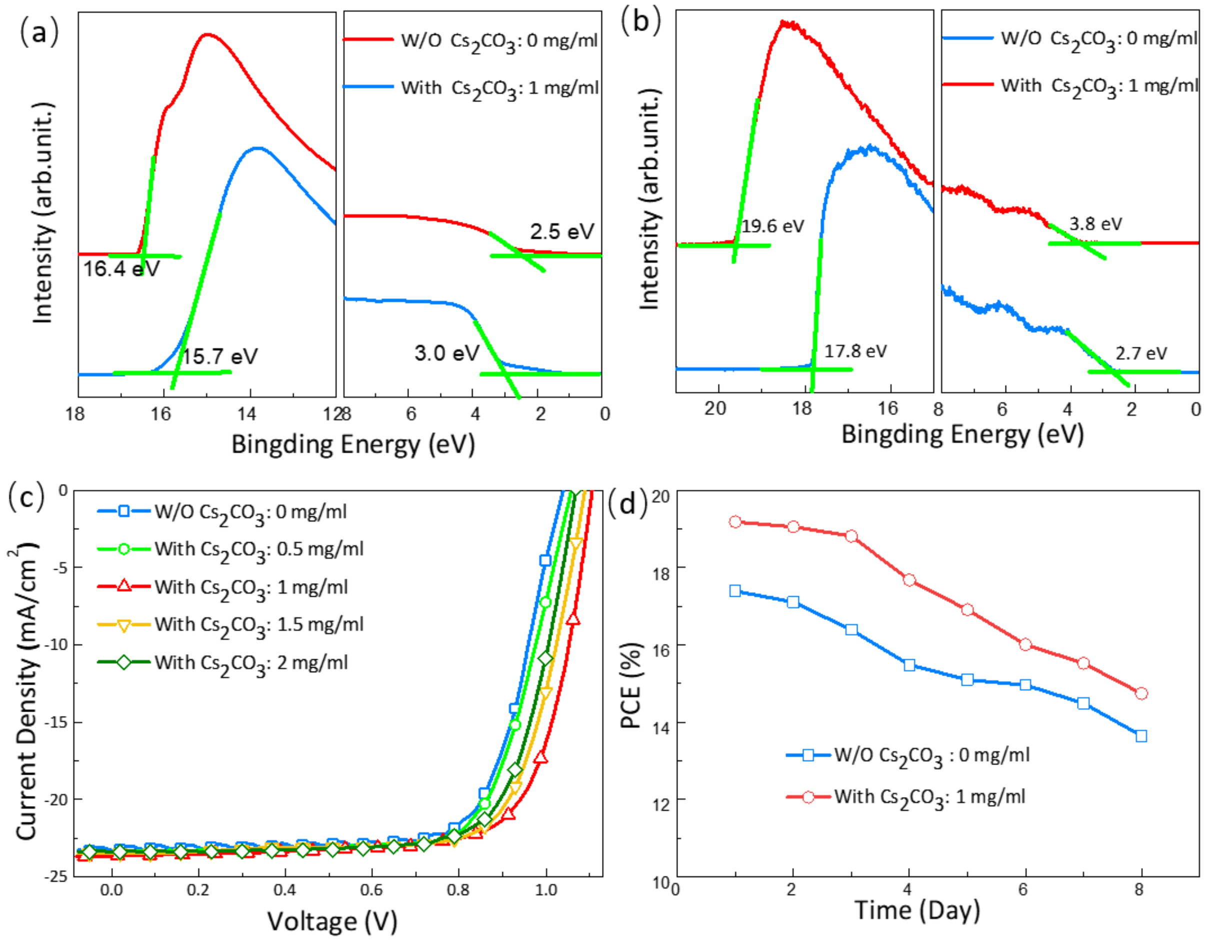

Fig. 5. (a) UPS spectra of TiO_2 layer with or without Cs_2CO_3 modification. (b) UPS spectra of $CH_3NH_3PbI_3$ layer on both TiO_2 layers. (c) *J*–*V* curves of the different devices under AM 1.5G illumination of 100 mW cm^{-2}. (d) The stability of devices based on pristine and doped TiO_2.

Table 1. Photovoltaic parameters of perovskite solar cells with different concentrations of Cs_2CO_3 doped in the TiO_2 layer.

Cs_2CO_3	V_{oc} (V)	J_{sc} (mA/cm^2)	FF (%)	PCE (%)
W/O	1.04	23.23	0.72	17.39
0.5 mg/ml	1.06	23.38	0.72	17.84
1.0 mg/ml	1.11	23.68	0.73	19.19
1.5 mg/ml	1.09	23.50	0.73	18.69
2.0 mg/ml	1.07	23.39	0.73	18.26

- Cesium carbonate was used as a new dopant to modify the TiO_2 layer.
- The fabrication technique is almost the same as the traditional one.
- The mechanisms of the dopant and optimal conditions were investigated.
- 19% power conversion efficiency of planar perovskite solar cells were achieved with enhanced stability.
- This new low-cost dopant is an ideal approach for the improvement of perovskite solar cells.